



EFFECTS OF SHAPE, SIZE, AND AIR VELOCITY ON ENTRY LOSS FACTORS OF SUCTION HOODS

Hugh E. McLoone , Steven E. Guffey & James P. Curran

To cite this article: Hugh E. McLoone , Steven E. Guffey & James P. Curran (1993) EFFECTS OF SHAPE, SIZE, AND AIR VELOCITY ON ENTRY LOSS FACTORS OF SUCTION HOODS, American Industrial Hygiene Association Journal, 54:3, 87-94, DOI: [10.1080/15298669391354397](https://doi.org/10.1080/15298669391354397)

To link to this article: <https://doi.org/10.1080/15298669391354397>



Published online: 04 Jun 2010.



Submit your article to this journal [↗](#)



Article views: 12



View related articles [↗](#)



Citing articles: 1 View citing articles [↗](#)

EFFECTS OF SHAPE, SIZE, AND AIR VELOCITY ON ENTRY LOSS FACTORS OF SUCTION HOODS*

Hugh E. McLoone^a

Steven E. Guffey^b

James P. Curran^c

^aApple Computer, Inc., 10260 Burbub Rd., MS: 56A, Cupertino, CA 95014; ^bUniversity of Washington, School of Public Health and Community Medicine, Department of Environmental Health, MS: SC-34, Seattle, WA 98195; ^cHeadquarters Electronic Systems Division, Systems Safety, Hanscom AFB, MA 01731.

This study further elucidated the effects of air velocity, aspect ratio (face length to face width), and area ratio (face area to duct area) on entry loss factors of suction hoods. A full scale ventilation system was utilized to determine the entry loss factor attributable to each of 20 square and rectangular hoods with a 90° included angle. Static and velocity pressures were measured using Pitot tubes connected by tubing to piezoresistive pressure transducers and inclined tube manometers. The entry loss factor, F_h , is the ratio of hood total pressure loss to mean velocity pressure. Values of F_h determined in this study ranged from 0.17–1.85. The values of F_h were a hyperbolic function of area ratio with a region rapidly increasing change for area ratios less than 5. For area ratios greater than 5, the values of F_h approached an asymptote of 0.17. Among hoods with a given area ratio (e.g., 2.5, 5.1, or 10.2), values of F_h were independent of aspect ratio. To a limited extent, F_h values decreased as mean air velocities increased from 319–1770 m/min (1046–5807 feet/min).

Local exhaust ventilation systems are often installed to protect workers from hazardous airborne contaminants. Ventilation system design relies on accurate prediction of pressure losses of system components such as hoods, which are the subject of this study. Knowledge of pressure loss associated with hoods is mostly attributable to Allen D. Brandt and J. M. Dalla Valle who studied pressure losses

associated with many hood design parameters with a limited number of hoods.⁽¹⁻⁴⁾

Both the American Conference of Government Industrial Hygienists (ACGIH) in their *Industrial Ventilation—A Manual of Recommended Practice* and the American Society of Heating, Refrigerating & Air-Conditioning Engineers, Inc. (ASHRAE) in their *ASHRAE Handbook & Product Directory* cite Brandt's values for pressure losses for certain hood designs.^(5,6) However, Brandt's as well as Dalla Valle's study designs may not have accounted for nonuniform flow development at the pressure measurement locations near the hood entrance. Thus, Brandt and Dalla Valle may have inaccurately measured pressure.

Another possible source of error in Brandt's studies was that he did not account for the pressure loss from friction of air flowing down the straight duct. In contrast, for fully developed turbulent flow, this study did consider the pressure loss attributable to friction between hood and pressure measurement locations.

All rectangular and square hoods used in this study had a major taper angle of 45° for an included angle of 90°. In Brandt's research, only square hoods had a 45° taper angle. Some rectangular hoods had taper angles of 38.75°, 40.5°, 53.5°, and 54.5°. In Dalla Valle's studies, the largest taper angle was only 33.7°, and that for only one rectangular hood.⁽³⁾ Hoods with a 45° taper were chosen for this study on the basis of their suggested use in many ventilation designs.⁽⁵⁾ Yet, hoods with 45° tapers are not the most efficient. Taper angles between 20°–30° offer the least resistance to air flow.^(1,7)

The pressure loss associated with a hood entrance can be expressed as a fraction of velocity pressure:

$$F_h = -\frac{TP_h}{VP} \quad (1)$$

*This work was supported by NIOSH grant No. 215 OH 07087, an Industrial Hygiene Research Council research grant, and a research assistantship from the Department of Environmental Health, University of Washington.

TABLE I. Hood Dimensions and Entry Loss Factors

Hood Number	Major Taper Angle	Minor Taper Angle	Length [cm]	Width [cm]	Face			Mean Air Velocity [m/min]	Pipe Factor ^A	Entry Loss Factors, F_h , determined from static pressure measurements at ^A			
					Area [cm ²]	Area Ratio ^A	Aspect Ratio ^A			1 D	2.5 D	5 D	20 D
1801.5 ^B	45°	-20°	46.1	4.22	195	1.07	10.92	879	0.843	2.019	1.877	1.848	1.841
1803 ^B	45°	-14°	46.3	7.8	359	1.97	5.94	1065	0.842	0.778	0.629	0.603	0.632
1804	45°	-10°	46.0	10.0	460	2.52	4.60	1066	0.844	0.575	0.417	0.389	0.402
1808	45°	9°	46.4	20.1	931	5.10	2.31	1099	0.840	0.287	0.203	0.207	0.223
1809	45°	14°	46.2	22.7	1048	5.75	2.04	1120	0.852	0.223	0.161	0.152	0.182
1816	45°	40°	45.9	41.0	1879	10.30	1.12	1104 ^C	0.849 ^C	0.247 ^C	0.171 ^C	0.179 ^C	0.212 ^C
2402 ^B	45°	-12°	61.2	5.2	321	1.76	11.77	992	0.849	0.956	0.871	0.870	0.879
2403 ^B	45°	-9°	61.4	7.7	476	2.61	7.97	1045	0.839	0.539	0.464	0.454	0.485
2404	45°	-6°	61.4	10.2	624	3.42	6.02	1074	0.842	0.401	0.313	0.307	0.328
2406	45°	0°	61.2	15.3	936	5.13	4.00	1142	0.843	0.269	0.182	0.173	0.201
2412	45°	18°	61.3	30.4	1863	10.21	2.02	1107 ^C	0.847 ^C	0.211 ^C	0.151 ^C	0.152 ^C	0.181 ^C
2418	45°	34°	61.2	46.4	2839	15.56	1.32	1115 ^C	0.851 ^C	0.217 ^C	0.146 ^C	0.150 ^C	0.174 ^C
2424	45°	45°	61.0	60.9	3711	20.35	1.00	1137	0.852	0.234	0.155	0.171	0.187
3602 ^B	45°	-7°	92.0	5.7	526	2.88	16.14	1079	0.849	0.358	0.311	0.308	0.351
3603 ^B	45°	-6°	92.0	7.6	701	3.84	12.11	1091	0.846	0.367	0.318	0.325	0.374
3604	45°	-4°	92.3	10.2	944	5.19	9.05	1095 ^C	0.845 ^C	0.249 ^C	0.197 ^C	0.201 ^C	0.239 ^C
3606	45°	0°	92.1	15.2	1399	7.67	6.06	1100	0.850	0.279	0.190	0.183	0.215
3608	45°	4°	91.8	20.4	1875	10.28	4.50	1109 ^C	0.845 ^C	0.268 ^C	0.156 ^C	0.158 ^C	0.180 ^C
3618	45°	22°	91.6	45.8	4195	23.00	2.00	1107 ^C	0.841 ^C	0.203 ^C	0.135 ^C	0.142 ^C	0.179 ^C
3636	45°	45°	91.1	91.9	8379	45.93	0.99	1098	0.856	0.294	0.187	0.191	0.230
Plain	0°	0°	15.24	15.24	182	1.00	1.00	1128	0.836	1.666	0.925 ^D	0.904	0.885 ^E

^AUnitless.

^BCompound hoods with a small face area, expansion of the air behind the hood face, and further contraction into the duct.

^CMean values from two sets of measurements near 1100 m/min mean air velocity. Other values result of single set of measurements.

^DDetermined at 3.5 D rather than 2.5 D.

^EDetermined at 18.5 D rather than 20 D.

where: F_h = entry loss factor

TP_h = total pressure attributable to hood at hood throat

VP = mean velocity pressure inside duct.

Outside the hood, static pressure is zero relative to atmospheric pressure and the velocity pressure is negligible, so

$$TP_h = SP + VP - TP_f \quad (2)$$

where: SP = mean centerline static pressure inside the duct at a location downstream from hood throat

TP_f = estimate of pressure loss due to friction along straight duct between hood throat and point at which SP is measured.

Within the limitations of one major taper angle, this study focused on three parameters: area ratio (ratio of hood face area to duct area), aspect ratio (ratio of length to width of hood face), and mean air velocity. The role of area ratio and aspect ratio with regard to entry loss factors was investigated beyond previous research (Table I). Both Brandt's and Dalla Valle's investigations were limited with respect to the range of aspect ratios and area ratios.^(2,3) With regard to area ratio, Brandt's hoods ranged from 2–6.5. In this study, area ratios ranged from 1–46. With regard to aspect ratio, Brandt's hoods ranged only from 1–4. The hoods in this study included aspect ratios from 1–16. Lastly, the theory that F_h values are independent of mean air velocity was tested.⁽²⁾

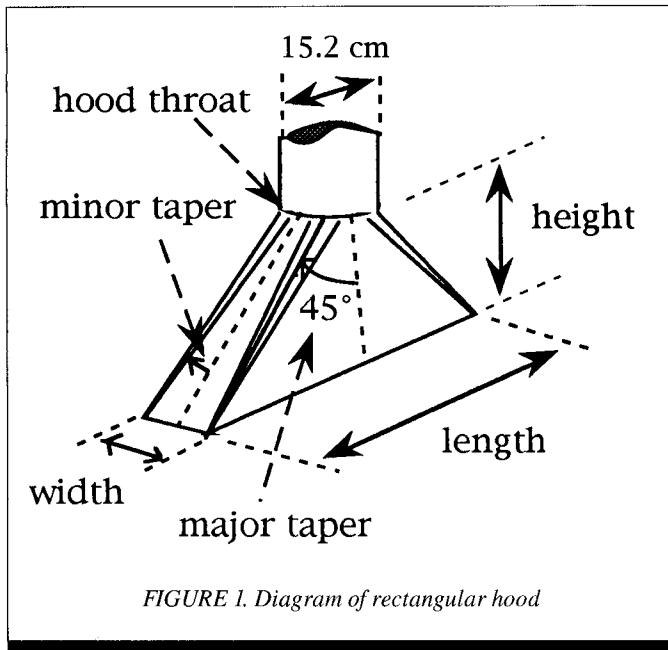
METHODS & MATERIALS

Hoods

The 20 square and rectangular hoods were constructed of 20-gauge (0.95 mm) galvanized sheet metal (Figure 1). The rectangular-to-round taper was constructed of identical halves that were spot welded together along the 45° taper angle sides. Another rectangular piece of sheet metal was rolled into a cylinder, which was spot welded to the round end of the hood section. The round portion fit snugly into the 15.2 cm (6 inch) diameter duct. The cylinder section added another 1.5 duct diameters (D) onto the end of the duct. No flanges or other surfaces circled the hood's face. However, wood frames were mounted on the outside of some hoods to force the flexible sheet metal sides into the designed shape and size. The frame's position away from the hood's edge did not affect pressure loss.⁽⁸⁾ Lastly, a plain hood (i.e., end of cut-off, spiral duct) also was utilized in this study.

Experimental Set-Up

The hoods were attached one at a time to a full-scale ventilation test system composed of ducting, supporting frame, fan, motor, and variable speed transmission. The fan's rotation rate was adjusted to provide the range of mean air velocities in the duct from 320–1770 m/min (1046–5807 feet/min). On



ceiling mounted frames, two separate branches of spiral wound ducts (3-meter [10-foot] lengths) were used to determine pressure losses due to friction along straight duct and each hood. The ducts were constructed of 24-gauge (0.635 mm) galvanized sheet metal. A prefabricated, internal, metal coupler joined the duct sections. The ducting was checked for levelness with a construction-type bubble level. Straightness was verified with a stringline. Thus, there was no contribution of gravity down the length of duct from the hood and no excess pressure losses due to non-straight duct.

After setup, holes were drilled at different locations along the duct to allow centerline static pressure measurements. For the hood testing setup, Pitot tube locations for static pressure measurements were 1, 2.5, 5, 20, and 40 D from the hood's throat. The terminus of the hood was considered to be the hood's throat, the beginning of the circular portion of the hood. For the friction setup, Pitot tube locations were 45.4, 61.8, 82.1, and 100.3 D from the hood's throat. Open holes were sealed with duct tape when a Pitot tube was not in place. In an attempt to assure the development of fully turbulent flow, the velocity pressure measurement station was located 46 D downstream of the hood's throat.

Pressure Measurement

Static and velocity pressures were measured using Pitot tubes connected by tubing to piezoresistive pressure transducers and inclined tube manometers. The 3.175 mm (0.125 in) diameter, hemispherical head Pitot tubes were held in place with specially designed Pitot tube holders.⁽⁹⁾ The piezoresistive pressure transducers utilized a sensing diaphragm with implanted resistors. Pressure applied to the diaphragm caused it to flex and, thus, resistance changed, resulting in a voltage proportional to pressure.⁽¹⁰⁾ The pressure transducers were utilized for velocity pressure measurements. An inclined tube manometer was used to measure static pressures. A personal

computer with data acquisition, spreadsheet and statistical programs was utilized to log velocity pressure measurements and perform data analysis.

Since the velocity of air flowing through the duct was not constant across a section and the Pitot tube indicated the velocity pressure at a point location, log-linear, 10-point Pitot tube traverses were performed along each of three diameters spaced 120° apart, for a total of 30 point velocity pressure.^(9,11) A point velocity was calculated from each velocity pressure using the inverse of Equation 3:

$$VP = df \left(\frac{V}{77.33} \right)^2 \quad (3)$$

where: VP = velocity pressure, point or mean, (Pascals [Pa])
V = velocity, point or mean, (m/min)

df = density factor: ratio of actual density to standard density.

Then, a mean air velocity was calculated from the 30 point velocities. Finally, the mean velocity pressure was determined from the mean velocity. Equation 3 assumed the standard density of dry air is 1.204 kg/m³ at 20° C and 760 mmHg.⁽¹²⁾

The density factor was computed using the ideal gas law:

$$df = \frac{(T_{std})(P_{act})}{(T_{act})(P_{std})} \quad (4)$$

where: T_{std} = standard temperature, 293.1 K

T_{act} = actual temperature, (K)

P_{std} = standard atmospheric pressure, 760 mmHg

P_{act} = actual atmospheric pressure, (mmHg)

Density factors were computed using the measured barometric pressure (corrected for temperature, latitude, and duct static pressure) and the duct air temperature. A psychrometer was used to measure the dew point depression. However, at the air temperatures present in the lab, the water vapor's content did not significantly change the density of air from standard, dry conditions.

Calibration of Instruments

Both the pressure transducers and inclined tube manometer were calibrated daily by comparison with pressure readings from a hook gauge. A hand pump, attached via tubing and connectors to the hook gauge, inclined manometer, and transducer(s), applied a range of pressure encompassing pressure to be measured that day.

Friction Model

The relationship between pressure loss due to friction along straight duct and mean air velocity was determined by conducting linear regression analysis following the model:⁽¹³⁾

$$\log \left(\frac{TP_f}{L} \right) = C_1 \log(V) + C_2 \quad (5)$$

where: TP_f = change in pressure due to friction (Pa)

L = length of duct between measurements (m)

V = mean air velocity (m/min)

C₁ and C₂ = regression coefficients

The log-log relationship was converted to an exponential relationship for ease of computations:

$$TP_f = C_3 L \left(\frac{V}{100} \right)^{C_1} \quad (6)$$

where: $\log(C_3) = 2C_1 + C_2$

RESULTS AND DISCUSSION

Fully Developed Turbulent Flow

The shape of the velocity profiles as represented by the magnitude of pipe factors suggested that turbulent air flow was fully developed at the VP measurement location 46 D from the hood throat. A pipe factor is the ratio of mean air velocity to centerline air velocity. For turbulent flow in smooth duct, pipe factors range from 0.82–0.84.^(6,11) As shown in Table I, pipe factors determined for square and rectangular hoods were consistent with fully developed, turbulent flow.

Friction

This study subtracted the contribution of friction (TP_f) from the pressure attributable to the hood (TP_h) and, ultimately, from the F_h values. Otherwise, the values of F_h would be conditional and arbitrary. The F_h values would vary greatly depending on the particular measurement location selected by the researcher or ventilation system engineer and on the roughness of the particular duct. Also, in ventilation system design procedures, friction losses are based on lengths measured “centerline-to-centerline” and other ventilation components such as elbows and tapers have “zero length” loss coefficients.^(5,6) If F_h values included a contribution due to an arbitrary duct length, design practice would have to be changed to subtract that length. If the additional duct length was not subtracted, the friction contribution would be overestimated. Thus, for simplicity and convenience, a length of zero (i.e., the hood throat) has been chosen as the point of reference for F_h values.

The pressure loss per length of straight duct increased exponentially with increasing mean air velocity (Figure 2). The pressure loss also increased with the number of couplers present per length of duct. Using Equation 6 for

the data shown in Figure 2, the change in pressure due to friction was modeled precisely by the following equations:

no couplers between pressure measurement locations ($R^2 = 0.999$),

$$TP_f = 0.249 L \left(\frac{V}{100} \right)^{1.84} \quad (7)$$

1 coupler per 5.6 m (18.4 feet) duct length ($R^2=0.999$),

$$TP_f = 0.259 L \left(\frac{V}{100} \right)^{1.83} \quad (8)$$

1 coupler per 3.8 m (12.5 feet) duct length ($R^2=1.000$),

$$TP_f = 0.271 L \left(\frac{V}{100} \right)^{1.83} \quad (9)$$

1 coupler per 2.9 m (9.5 feet) duct length ($R^2=1.000$),

$$TP_f = 0.292 L \left(\frac{V}{100} \right)^{1.82} \quad (10)$$

Equation 7 was used to estimate the pressure loss due to friction along the duct between the hood throat and the 20 D measurement location for F_h determinations, since there were no couplers in that stretch of duct.

Hoods are known to affect the pressure loss due to friction along straight duct near the hood throat. For a bell-mouth entry, pressure loss along straight duct was found to be 20%

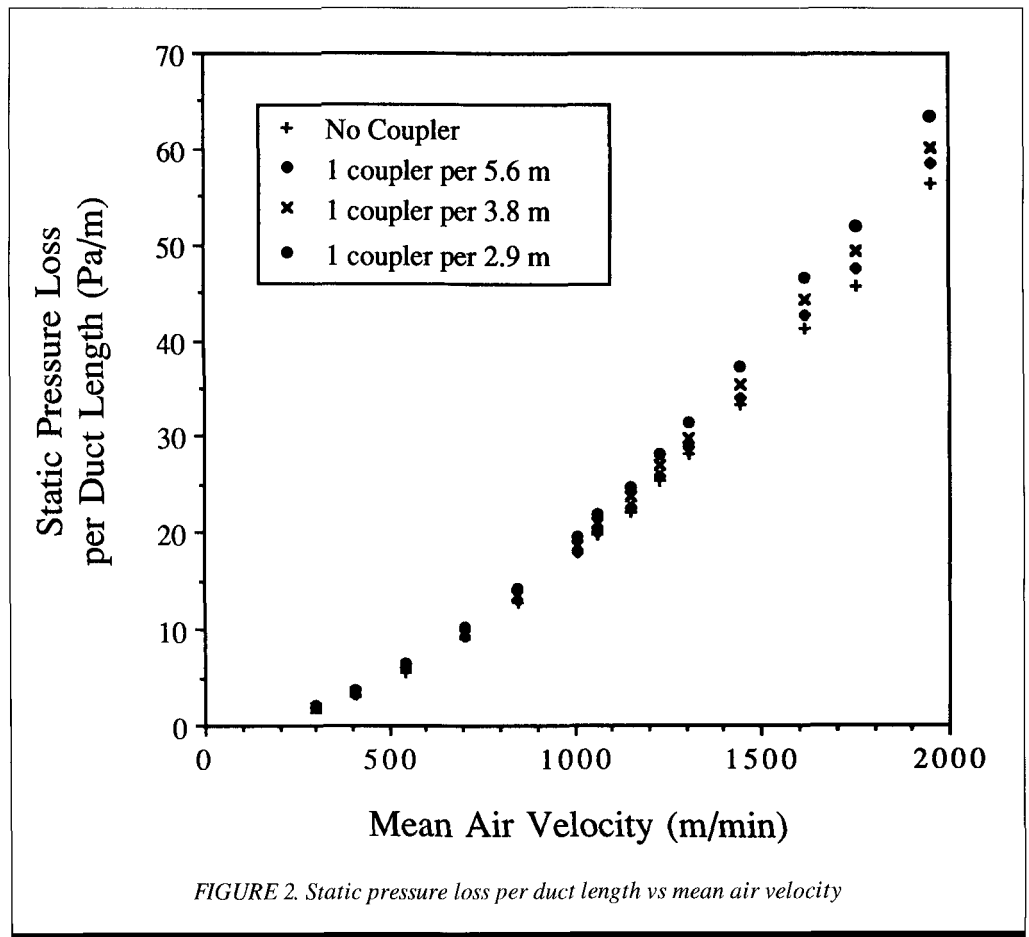


FIGURE 2. Static pressure loss per duct length vs mean air velocity

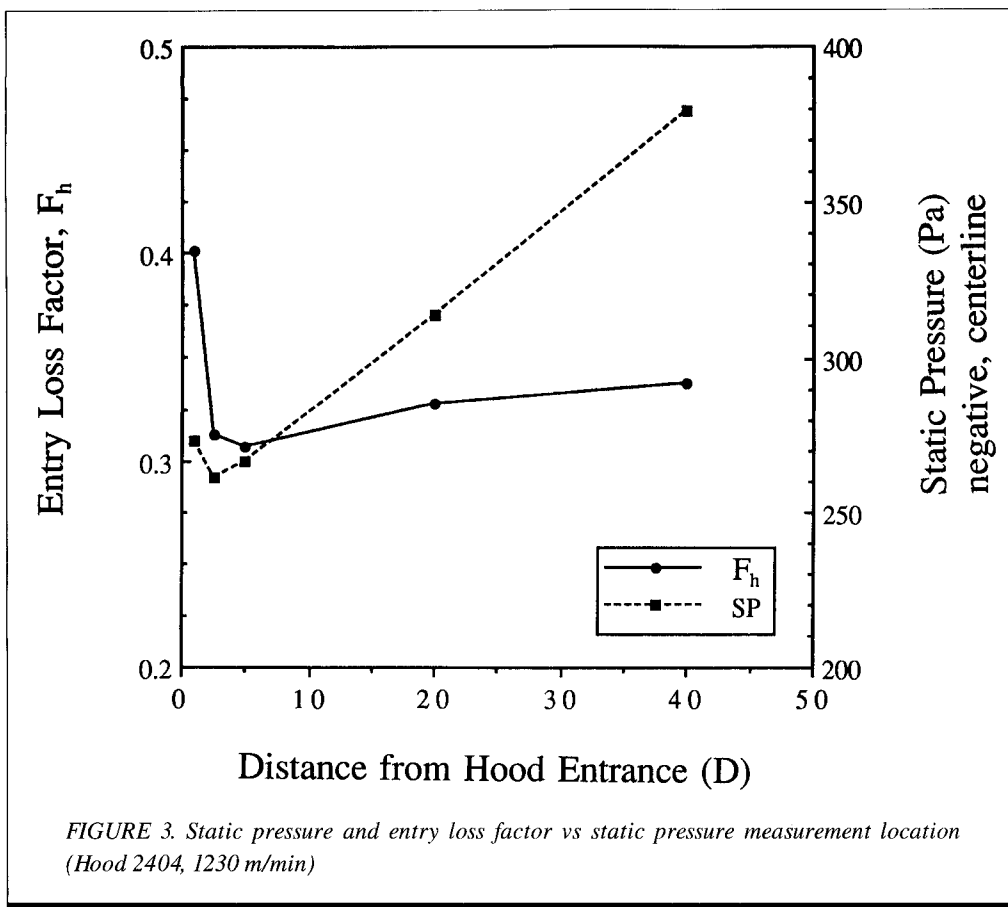


FIGURE 3. Static pressure and entry loss factor vs static pressure measurement location (Hood 2404, 1230 m/min)

higher at 2 D, 10% higher at 5 D, and 4% higher at 10 D when compared to pressure loss in fully developed flow.⁽¹⁴⁾ Static pressure gradients attained their fully developed values within the first 15 D. However, Barbin and Jones promoted turbulence artificially using sand grains glued to the pipe wall near the entrance. This study did not use sand grains and found that the effect of the hood entrance on static pressure gradients may extend beyond 20 D for relatively smooth duct surfaces. The measured static pressure losses between 5 D and 20 D were 10%–11% greater than values predicted using the estimated friction of fully developed flow (Equation 7). The measured static pressure differences between 20 and 40 D were 3% higher than the predicted pressure loss due to friction (Equation 10). This small pressure loss difference between 20 D and 40 D may be the result of hood entrance effects far downstream or the fact that different couplers were used or both. Even though the same type of coupler was used for the friction modeling and hood testing, individual couplers differed measurably in the magnitude of their pressure loss.⁽⁸⁾

Entry Loss Factors

For each hood, the total pressure loss attributable to the hood, TP_h , was determined from the measured static and velocity pressures and the estimated contribution of friction between the static pressure measurement location and the hood throat, using Equation 2. The entry loss factor was determined from Equation 1. For SP measurement locations of 1, 2.5, 5, and 20 D for rectangular and square hoods and 1, 3.5, 5,

and 18.5 D for the plain hood, the F_h values determined are shown in Table I.

Distance from Hood Throat

The magnitude of static pressure depended on the distance downstream from the hood throat. As shown in Figure 3, the magnitude of the static pressures measured at centerline was less at 2.5 D than at 1 D. Further downstream, static pressure began a steady increase in magnitude as air flowed down the duct. Likewise, F_h values were highest when based on SP measurements at 1 D, dropped to a lower value at 2.5 D, and then increased slightly with increasing distance from the hood. The increase in magnitude of static pressures beyond 5 D was the result of pressure loss due to friction along straight duct. The decrease in static pressure between 1 and 2.5 D was the result of the *vena contracta*, which reduces the effective size of the duct opening and increases mean velocity pressure and thus makes centerline static pressure more negative.^(5,6,15) Despite correcting for friction pressure losses, values of F_h did not appear to reach a maximum plateau even after 20 D.

This effect of SP measurement distance from hood throat on F_h values was not consistent with Brandt's conclusions. From wall static pressures measured at locations less than or equal to 5 D, Brandt found very little effect of pressure measurement distance from hood throat on F_h values, even a 1 D.⁽²⁾ However in this study, the wall static pressures near the hood throat were less than mean static pressure.⁽⁸⁾ The magnitude of the difference between wall SP and mean SP decreased with distance from the hood throat. Near 5 D, wall static pressure equaled mean static pressure. At the same time, friction along straight duct was small—but not zero. Since Brandt measured SP only at the wall, Brandt may have overlooked the balance between nonuniform static pressure profiles and friction along straight duct.

With the exception of the 18.5 D location for the plain hood, static pressure measurement locations closer than 20 D were not utilized for comparing F_h values to hood size, hood shape, and mean air velocity. Static pressure traverse profiles were not uniform and friction along straight duct had not achieved constant pressure loss per duct length.⁽⁸⁾ The 40 D location was not selected since the friction loss associated with the coupler could not be estimated accurately. Ventilation system designers use estimates of friction predicted from

With the exception of the 18.5 D location for the plain hood, static pressure measurement locations closer than 20 D were not utilized for comparing F_h values to hood size, hood shape, and mean air velocity. Static pressure traverse profiles were not uniform and friction along straight duct had not achieved constant pressure loss per duct length.⁽⁸⁾ The 40 D location was not selected since the friction loss associated with the coupler could not be estimated accurately. Ventilation system designers use estimates of friction predicted from

fully developed turbulent flow along straight duct from the hood throat.⁽⁵⁾ This estimate of friction does not include the hood's additional contribution to pressure losses. Yet, the F_h values determined at 20 D do and are recommended for the design of ventilation systems.

Aspect Ratio

Values of F_h appeared to be independent of the relative dimensions of length and width. Values of F_h did not consistently increase or decrease with aspect ratio for three rectangular hoods within three sets of area ratios near 2.6, 5.1, and 10.3 (Table I). This result could not be compared with Brandt's research since his hoods did not include any hoods where area ratio and taper angle were held constant while aspect ratio was varied.

Area Ratio

Area ratio did significantly affect entry loss factors. As shown in Figure 4, values of F_h increased with decreasing area ratios below 5 and decreased to a minimum, stable value of approximately 0.18 for area ratios above 5. Thus, there was a minimum entry pressure loss attributable to rectangular hoods regardless of the face area's size relative to duct size. Conversely, as the face area of the hood becomes progressively smaller relative to the duct area, hood entry loss factors increased rapidly. The cause of this increase in entry loss factors was probably two-fold. First, the small face area did not provide as gradual a transition to direct air into the duct compared to larger face area ratios. Compared to the shape of larger hoods, smaller hoods' shape produced a large *vena contracta* as air flowed into the duct. So, pressure loss would increase as the VP at the *vena contracta* was converted to SP as air filled the duct.⁽⁵⁾ Second, some rectangular hoods with small area ratios behaved like compound hoods with a slot at the face (i.e., aspect ratios > 5). The maximum hood cross-sectional area was not at the face but rather was in the interior of the hood. Air accelerated initially from outside to inside the hood, decelerated inside the hood as the cross-sectional area increased, and then accelerated again as air flowed into the ducting with smaller cross-sectional area. All three of the changes in velocity contributed to pressure losses.

The independence of entry loss factors for area ratios ≥ 5 conflicts with Brandt's research and ACGIH's use of Brandt's research in their *Industrial Ventilation*. Brandt stated that F_h

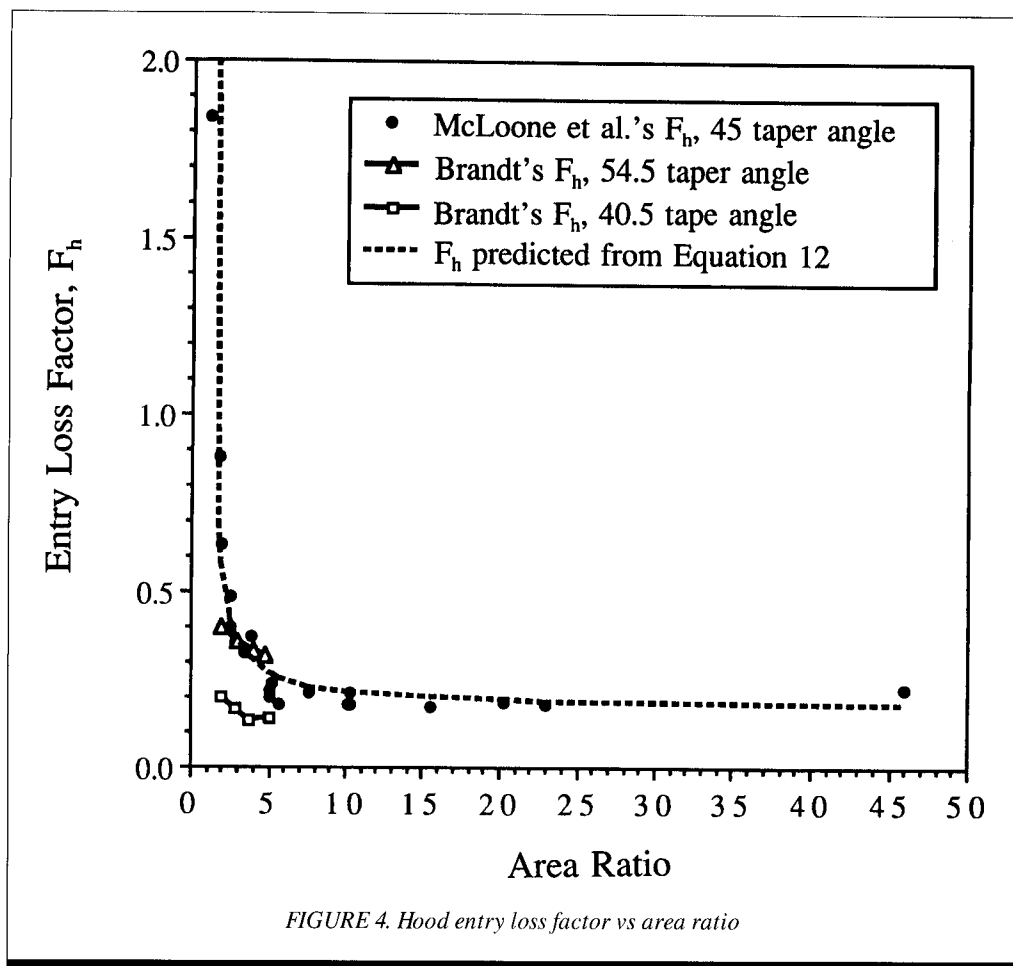


FIGURE 4. Hood entry loss factor vs area ratio

values were independent for area ratios ≥ 2 .⁽²⁾ Yet, even Brandt questioned his own findings:

at first glance it would seem that face area to throat area should have an influence on the coefficient since the loss at the hood face obviously is greater with a small than with a large area and it seems unlikely that this difference is made up by the greater length of the larger area hood. It is hoped that this problem may be investigated further to find the reason for these results.⁽²⁾

The limited sizes of Brandt's hoods prevented him from observing the steep rise in F_h as area ratios decreased and the minimum, stable value in F_h as area ratios increased.

The results of this study can be compared to Brandt's findings by selecting sets of hoods with taper angles larger and smaller than the 45° taper angle used in this study. For sets of hoods with taper angles of 40.5° and 54.5°, Brandt's values straddle the hood loss factors determined in this study with taper angles of 45° (Figure 4). This result was expected since hood losses increased with increasing taper angles above 20°.⁽²⁾

In this study, values of F_h appeared to be inversely proportional to the area ratio squared,

$$F_h = \frac{C}{(AR)^2} + F_{h\infty} \quad (11)$$

where AR = area ratio
 $F_h = F$, at area ratio of infinity
 C = regression coefficient

From empirical data for F_h values at 20 D and corresponding area ratios, the following relationship was determined and plotted against measured values in Figure 4.

$$F_h = \frac{1.9}{(AR)^2} + 0.17 \quad (12)$$

Equation 12 applies only to square and rectangular hoods with a major included angle of 90°.

Air Velocity

The values of F_h for most hoods were determined at mean air velocities near 1100 m/min (3608 feet/min), ranging from 990–1160 m/min (3247–3805 feet/min). An exception was hood number 1801.5 whose F_h was determined at 880 m/min (2886 feet/min). To determine the validity of the assumption that F_h was independent of velocity, values of F_h for three hoods—3618, 2404, and plain—were checked at a range of air velocities from 319 m/min (1046 feet/min) to 1770 m/min (5807 feet/min). For all three hoods, the F_h values were not constant with velocity (Figure 5). Rather, the F_h value appeared to decrease with increasing air velocity, except for the lowest velocities tested. Pressures were too low (< 25 Pa [< 0.10 inch water gauge]) for accurate estimation of F_h at

low air velocities, as shown by the large standard deviations at these velocities. For mean air velocities greater than 500 m/min (1640 feet/min), a strong negative correlation was seen between mean air velocity and entry loss factors. The (Pearson) correlation coefficient was -0.944 ($p < 0.01$), -0.882 ($p < 0.001$), and -0.780 ($p < 0.001$) for the plain, 2404, and 3618 hoods, respectively. Increasing the mean air velocity from 500 m/min (1640 feet/min) to 1500 m/min (4920 feet/min) resulted in a 0.11 (12%), 0.06 (16%), and 0.04 (19%) decrease in F_h for the plain, 2404, and 3618 hoods, respectively.

Brandt found entry loss factors to be independent of mean air velocity for 70 hoods tested at velocities between 610 m/min (2000 feet/min) and 1524 m/min (5000 feet/min).⁽²⁾ Brandt averaged the 70 entry loss factors for each velocity tested. This mean F_h value of all hoods was reported by Brandt to be constant regardless of air velocity. No individual hood results were given.

The effect of velocity on F_h values could be expected considering the local effect of the hood on pressure loss due to friction. As previously discussed, friction loss factors varied with distance from the throat, yet the estimate of pressure loss due to friction was based on friction loss per length of duct determined at distances more than 40 D downstream from hood throat. Since the friction loss varied with $V^{1.82}$ to $V^{1.84}$ (Equations 7 to 10) and dynamic losses vary with V^2 (Equation 3), any error in the friction estimate would vary with velocity.

Therefore, just on the basis of friction considerations, the error of F_h will vary inversely with $V^{0.16}$ to $V^{0.18}$ and the estimated F_h will decrease with increasing velocity. If the local effect of the hood on friction was completely and correctly estimated, the actual value of F_h could be constant with velocity. However, this study did not attempt to separate or estimate the local effect of the hood on friction (and no attempt is made in the field). So, the local effect of the hood on friction remained confounded with the dynamic losses of the hood.

CONCLUSION

The entry loss factors, F_h , were determined for twenty square and rectangular hoods with a major included angle of 90°. The F_h values range from 0.17–1.85. The F_h values were independent of aspect ratio and dependent on area ratio. Entry loss factors decreased with increasing air velocity—approximately

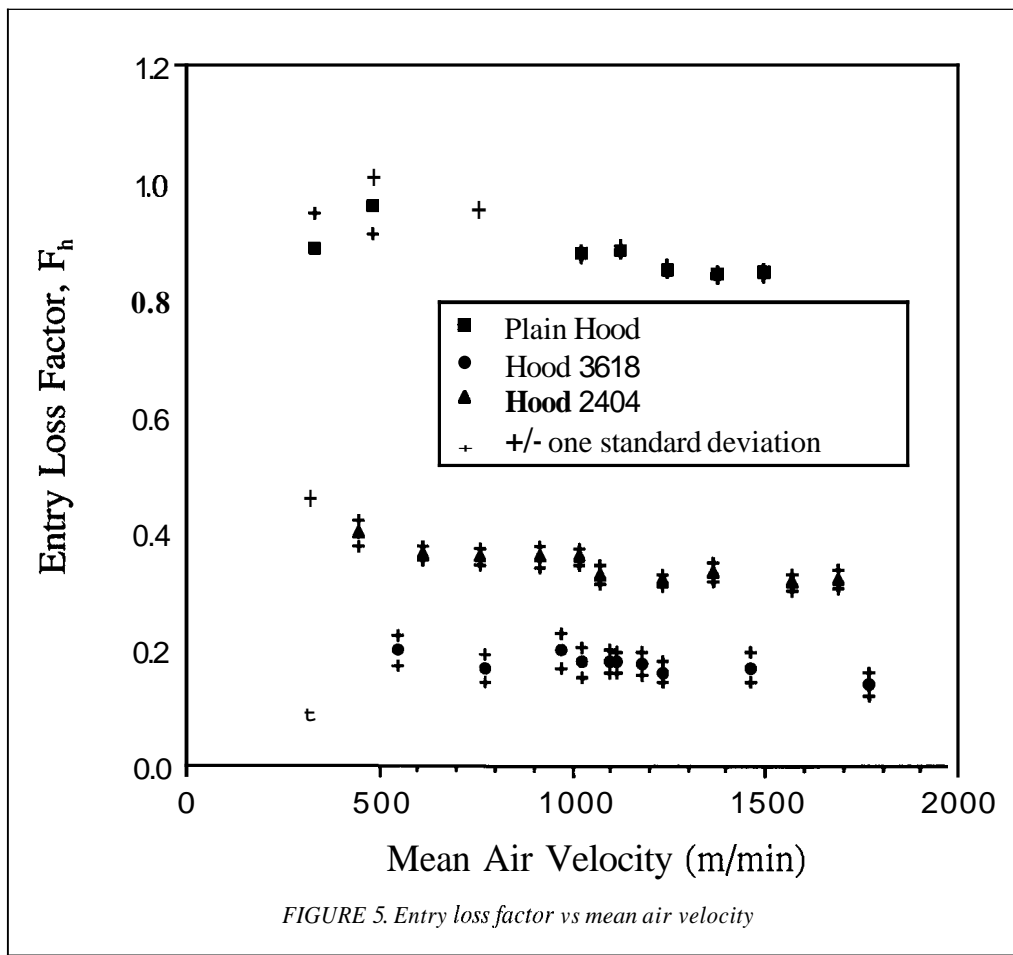


FIGURE 5. Entry loss factor vs mean air velocity

1%–2% per 100 m/min (328 feet/min) increase in mean air velocity, possible due to the hood's effect on pressure loss due to friction along straight duct beyond the hood throat.

The results of this study were consistent with the values of entry loss factors determined in Brandt's research. However, this study found mean air velocity and SP measurement location did affect the magnitude of F_h values whereas Brandt's research did not. Future investigations may develop descriptive relationships between F_h and area ratio for hoods with different shapes and different taper angles.

REFERENCES

1. **Brandt, Allen D.:** A Summary of Design Data for Exhaust Systems. *Heat. Vent.* 42:73-88 (1945).
2. **Brandt, Allen D. and Russell J. Steffy:** Energy Losses at Suction Hoods. *Heating, Piping & Air Conditioning—Am. Soc. Heat. Vent. Eng. J. Section. Sept:*105-119 (1946).
3. **Dalla Valle, J.M.:** How to Design Exhaust Hoods, Part 11—Hood Entrance Losses. *Heat. Vent.* 41:61 (1943).
4. **Dalla Valle, J.M.:** *Exhaust Hoods.* New York: The Industrial Press, 1962.
5. **American Conference of Governmental Industrial Hygienists, Committee on Industrial Ventilation:** *Industrial Ventilation, 20th Edition, A Manual of Recommended Practice.* Cincinnati, OH: ACGIH, 1988.
6. **American Society of Heating, Refrigerating & Air-conditioning Engineers, Inc.:** *ASHRAE Handbook & Product Directory, 1989—Fundamentals.* Atlanta, GA: ASHRAE, 1985.
7. **Idelchik, I.E.:** *Handbook of Hydraulic Resistances, Second Edition, Revised and Augmented.* New York: Hemisphere Publishing Corp., 1986.
8. **McLoone, Hugh E.:** "Pressure Loss of Air Flowing into Square and Rectangular Hoods." M.S. thesis, University of Washington, 1990.
9. **Guffey, Steven E.:** Simplifying Pitot Traverses. *Appl. Occup. Environ. Hyg.* 5(2):95-100 (1990).
10. **Omega Engineering, Inc.:** *Series PX160 Pressure Transducer Data Sheet.* Stamford, CT: Omega Engineering, Inc., 1988.
11. **Ower, E. and R. C. Pankhurst:** *The Measurement of Air Flow.* London: Pergamon Press Ltd., 1966.
12. **Pines, David, ed.:** Physical and Numerical Constants. *Rev. Mod. Phys.* 52(2): S33, (1980).
13. **Guffey, Steven E.:** Friction Tables Determined from Colebrook's Equation for Standard Density Air Flow. *Appl. Occup. Environ. Hyg.* (In Press).
14. **Barbin, A. R. and J. B. Jones:** Turbulent Flow in the Inlet Region of Smooth Pipe. *J. Basic Eng. March:*29-34 (1963).
15. **Ward-Smith, A. J.:** *The Fluid Dynamics of Flow in Pipes and Ducts.* Oxford: Clarendon Press, 1980.